

# Self-Assembled Three-Dimensional Graphene Macrostructures: Synthesis and Applications in Supercapacitors

Yuxi Xu,<sup>§</sup> Gaoquan Shi,<sup>\*,#</sup> and Xiangfeng Duan<sup>\*,§</sup>

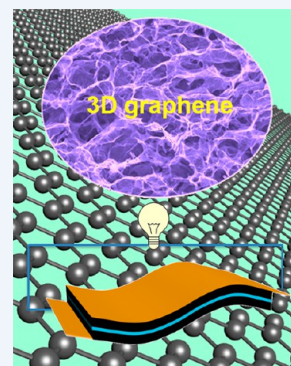
<sup>§</sup>Department of Chemistry and Biochemistry, University of California, Los Angeles, California 90095, United States

<sup>#</sup>Department of Chemistry, Tsinghua University, Beijing 100084, China

**CONSPECTUS:** Graphene and its derivatives are versatile building blocks for bottom-up assembly of advanced functional materials. In particular, with exceptionally large specific surface area, excellent electrical conductivity, and superior chemical/electrochemical stability, graphene represents the ideal material for various electrochemical energy storage devices including supercapacitors. However, due to the strong  $\pi$ - $\pi$  interaction between graphene sheets, the graphene flakes tend to restack to form graphite-like powders when they are processed into practical electrode materials, which can greatly reduce the specific surface area and lead to inefficient utilization of the graphene layers for electrochemical energy storage. The self-assembly of two-dimensional graphene sheets into three-dimensional (3D) framework structures can largely retain the unique properties of individual graphene sheets and has recently garnered intense interest for fundamental investigations and potential applications in diverse technologies.

In this Account, we review the recent advances in preparing 3D graphene macrostructures and exploring them as a unique platform for supercapacitor applications. We first describe the synthetic strategies, in which reduction of a graphene oxide dispersion above a certain critical concentration can induce the reduced graphene oxide sheets to cross-link with each other via partial  $\pi$ - $\pi$  stacking interactions to form a 3D interconnected porous macrostructure. Multiple reduction strategies, including hydrothermal/solvothermal reduction, chemical reduction, and electrochemical reduction, have been developed for the preparation of 3D graphene macrostructures. The versatile synthetic strategies allow for easy incorporation of heteroatoms, carbon nanomaterials, functional polymers, and inorganic nanostructures into the macrostructures to yield diverse composites with tailored structures and properties. We then summarize the applications of the 3D graphene macrostructures for high-performance supercapacitors. With a unique framework structure in which the graphene sheets are interlocked in 3D space to prevent their restacking, the graphene macrostructures feature very high specific surface areas, rapid electron and ion transport, and superior mechanical strength. They can thus be directly used as supercapacitor electrodes with excellent specific capacitances, rate capabilities, and cycling stabilities. We finally discuss the current challenges and future opportunities in this research field.

By regarding the graphene as both a single-atom-thick carbon sheet and a conjugated macromolecule, our work opens a new avenue to bottom-up self-assembly of graphene macromolecule sheets into functional 3D graphene macrostructures with remarkable electrochemical performances. We hope that this Account will promote further efforts toward fundamental investigation of graphene self-assembly and the development of advanced 3D graphene materials for their real-world applications in electrochemical energy storage devices and beyond.



## 1. INTRODUCTION

Graphene, a monolayer of graphite, has shown a wide range of promising applications, including electronic devices, energy storage and conversion, and polymer composites, since its first isolation in 2004.<sup>1-6</sup> Several methods such as mechanical exfoliation, chemical vapor deposition, and reduction of graphene oxide (GO) have been widely explored to produce graphene for fundamental and applied research.<sup>1-8</sup> Among these, reduction of GO has attracted particular interest in the chemistry and materials communities because of its capability for low-cost and high-throughput production of reduced graphene oxide (RGO).<sup>8</sup> It is recognized that controlled preparation of graphene materials with well-defined hierarchical structures will pave the way for many practical applications that need bulk graphene materials. Self-assembly can be expected to be an effective technique for this purpose, which is capable of

organizing building blocks into complex architectures via hydrogen bonding,  $\pi$ - $\pi$  stacking interactions, electrostatic forces, etc. As the precursor of RGO, GO prepared by chemical oxidation of graphite can be well dispersed in many polar solvents, especially in water, at high concentrations and can be easily converted into RGO with largely restored conjugation by diverse reduction methods.<sup>8</sup> Therefore, GO and RGO sheets can be regarded not only as carbon nanomaterials but also as two-dimensional (2D) conjugated macromolecules with extremely large molar masses based on their micrometer- or submicrometer-scale lateral sizes and naturally become versatile building blocks for the self-assembly of advanced materials with designed superstructures and functions.<sup>9-19</sup>

Received: March 9, 2015

Published: June 4, 2015



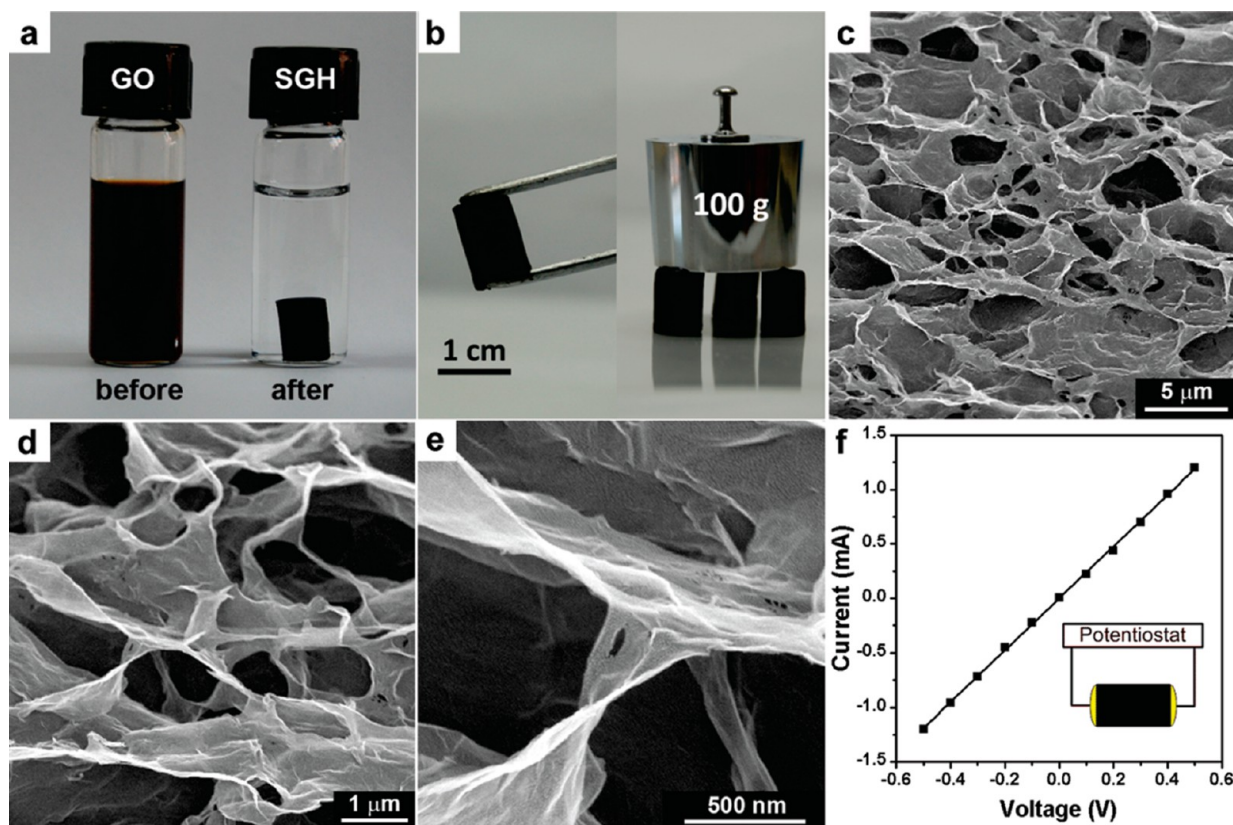


**Figure 1.** (a) Photographs of a 2 mg/mL homogeneous GO aqueous dispersion before and after hydrothermal reduction at 180 °C for 12 h. (b) Photographs of a strong graphene hydrogel allowing easy handling and weight support. (c–e) Scanning electron microscope (SEM) images with different magnifications of the graphene hydrogel's interior microstructures. (f) Room temperature  $I$ – $V$  curve of the graphene hydrogel exhibiting Ohmic characteristics. Inset shows the two-probe method for the conductivity measurements. Reproduced with permission from ref 28. Copyright 2010 American Chemical Society.

Electrochemical energy storage devices are of great importance for mobile electronics, electrical vehicles, and renewable energy harvesting, conversion, and storage.<sup>20</sup> Graphene has attracted considerable interest in this regard because of its multiple appealing features, including high specific surface area, excellent electrical conductivity, and extraordinary chemical/electrochemical stability and mechanical flexibility.<sup>21</sup> However, the strong van der Waals and  $\pi$ – $\pi$  stacking interactions between graphene sheets make them readily aggregate to form graphite-like powders with compact layered structures when processed into bulk electrode materials, leading to a great loss of specific surface area and thus inefficient utilization of graphene layers for electrochemical energy storage. Moreover, electrochemically inactive polymer binders and/or conductive additives are usually needed to combine these graphite-like graphene powders into practical electrodes, which not only complicates the electrode preparation process but also introduces additional loss in the electrochemical performance.

Self-assembly of nanoscale graphene into monolithic macroscopic materials with three-dimensional (3D) porous networks can largely translate the properties of individual graphene into the resulting macrostructures and simplify the processing of graphene materials. It has therefore garnered intense interest in the past few years.<sup>22–27</sup> In this Account, we will present our recent advances in developing synthetic strategies to prepare 3D self-assembled graphene macrostructures starting with GO and exploring these materials for the creation of supercapacitors with unprecedented performance.

## 2. SYNTHETIC STRATEGIES

### 2.1. Hydrothermal or Solvothermal Reduction

We have synthesized the first self-assembled 3D graphene macrostructure, that is, graphene hydrogels, in 2010. The graphene hydrogel was produced by a convenient one-step hydrothermal reduction of a highly concentrated GO aqueous dispersion (Figure 1).<sup>28</sup> A typical graphene hydrogel consists of a highly interconnected 3D graphene network ( $\sim 2$  wt %) filled with water ( $\sim 98$  wt %). The pore sizes in the 3D graphene range from submicrometer to several micrometers, and pore walls consist of thin layers of stacked graphene sheets. We proposed the self-assembly mechanism as follows: before reduction, the separated GO sheets were randomly and uniformly dispersed in water, due to their strong hydrophilicity and electrostatic repulsion effect. When GO was hydrothermally reduced, the oxygenated functionalities decreased significantly and the  $\pi$ -conjugation was largely restored. The  $\pi$ – $\pi$  stacking interaction combined with hydrophobic effect promoted flexible RGO sheets to partially overlap and interlock with each other in 3D space to generate enough physical cross-link sites for the formation of a porous framework with water entrapped inside.

Due to the unique self-assembled structure and superior graphene building block, the graphene hydrogel showed a high electrical conductivity of 0.5 S/m, a hierarchical meso- and macroporosity with a large specific surface area of 960 m<sup>2</sup>/g, and excellent mechanical strength with a storage modulus of 450–490 kPa, which is about 1–3 orders of magnitude higher

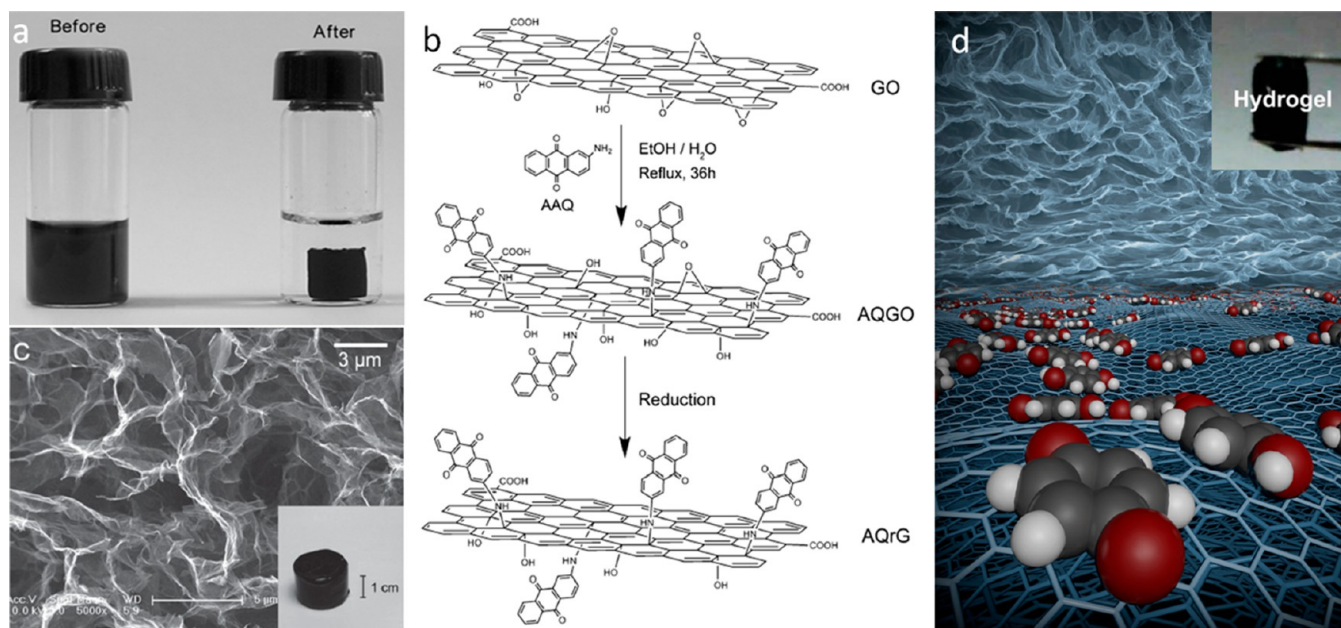


**Figure 2.** (a) Photograph of an aqueous mixture of GO (2 mg/mL) and sodium ascorbate before (left) and after (right) chemical reduction at 90 °C for 1.5 h. Reproduced with permission from ref 46. Copyright 2011 Elsevier Ltd. (b) Schematic illustration of synthesis of anthraquinone-grafted graphene hydrogel. (c) SEM image of anthraquinone-modified graphene hydrogel and its photograph shown in the inset. Reproduced with permission from ref 49. Copyright 2011 Royal Society of Chemistry. (d) Schematic illustration of hydroquinone functionalized graphene hydrogel and its photograph shown in the inset. Reproduced with permission from ref 50. Copyright 2013 Wiley-VCH.

than those of conventional self-assembled hydrogels. This initial study provides a new fundamental understanding of the self-assembly mechanism of graphene as a 2D macromolecule building block and inspires abundant subsequent studies on 3D graphene macrostructures. Soon after this work, we further used solvothermal reduction to prepare self-assembled graphene organogel starting with a GO dispersion in propylene carbonate.<sup>29</sup> The graphene organogel showed similar porous network and mechanical strength and even a higher electrical conductivity of 2 S/m. These graphene hydrogels/organogels can be easily converted into graphene aerogels by using a freezing-drying or supercritical drying process.

The hydrothermal and solvothermal reduction strategies are the most direct route to produce graphene gels without introducing any other chemicals or further purification treatment. Additionally, these processes are compatible with synthesis of many functional materials, which allows for convenient incorporation of a variety of secondary components into the 3D graphene framework to tailor the structures and combine the functions of multiple components. For example, we have demonstrated a one-step hydrothermal approach for the synthesis of graphene/Ni(OH)<sub>2</sub> composite hydrogels by using an aqueous mixture of GO and nickel nitrate as the starting materials.<sup>30</sup> The hydrothermal process not only induced the 3D self-assembly of graphene but also simultaneously promoted uniform in situ growth of ultrathin crystalline Ni(OH)<sub>2</sub> nanoplates on the graphene framework. Utilizing the amphiphilic feature of GO, we have dispersed activated carbon particles into propylene carbonate and prepared graphene/activated carbon composite organogels by solvothermal reduction of the mixture dispersion.<sup>31</sup> The resulting organogels consisted of a 3D graphene porous network with encapsulated carbon particles. Other research groups have also synthesized heteroatom-doped graphene hydrogels/aerogels,<sup>32–34</sup> graphene/carbon nanotubes,<sup>35,36</sup> gra-

phene/polymers,<sup>37,38</sup> graphene/metal nanoparticles,<sup>39–41</sup> and graphene/metal oxide and sulfide<sup>42–44</sup> composite hydrogels/aerogels using the hydrothermal or solvothermal reduction strategies, which greatly expand the diversity and functions of 3D self-assembled graphene macrostructures. More recently, we have prepared a new 3D graphene macrostructure built from holey graphene sheets through a one-step hydrothermal process with simultaneous etching of nanopores within the graphene plane and self-assembly of graphene into a 3D network, which exhibited a highly continuous porous network of open channels with a ultrahigh accessible surface area of 1560 m<sup>2</sup>/g.<sup>45</sup>

## 2.2. Chemical Reduction

Although the hydrothermal or solvothermal strategies have their own features, the reactions require high temperature and high pressure, which is time-consuming and energy-consuming. Therefore, a milder method is needed for producing 3D self-assembled graphene macrostructures in large scale. Recognizing that the self-assembly of individual graphene sheets into a 3D network is mainly induced by the increased  $\pi$ - $\pi$  stacking interaction between RGO during the hydrothermal reduction process, it is reasonable to believe that a chemical reduction process could also initiate the self-assembly of the 3D graphene network. Indeed, we have successfully synthesized graphene hydrogels by using sodium ascorbate as a reducing agent in the GO aqueous dispersion (Figure 2a).<sup>46</sup> In contrast to the high temperature (180 °C) and long time (12 h) used in hydrothermal reduction, the chemical reduction process can be completed within less than 2 h below 100 °C. Moreover, the reaction is not limited to the autoclaves used in hydrothermal reduction and the shape of the graphene hydrogels can be easily varied by changing the type of reactor.

The graphene hydrogels prepared by chemical reduction showed similar porous structure and mechanical properties. It is notable that their electrical conductivity (1–2 S/m) is higher

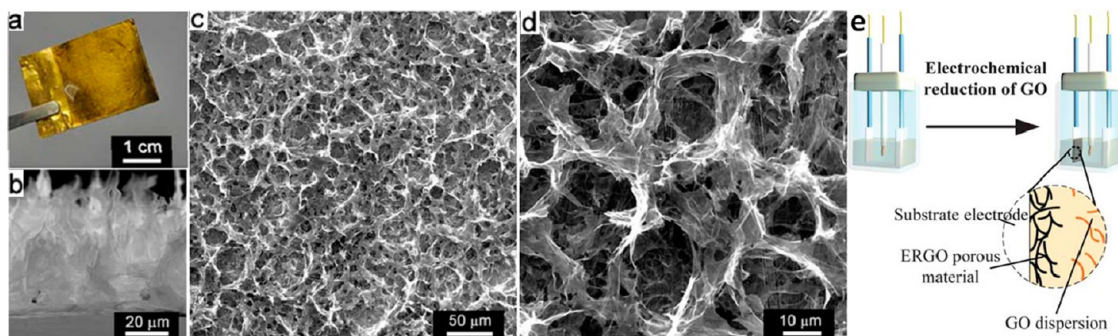


**Figure 3.** Photograph (a) and cross-sectional SEM image (b) of an electrodeposited graphene hydrogel thin film electrode. (c, d) Top-view SEM images with low (c) and high (d) magnifications. Reproduced with permission from ref 54. Copyright 2012 Nature Publishing Group. (e) Schematic illustration of the electrochemical reduction method for producing graphene hydrogel film on electrode. Reproduced with permission from ref 55. Copyright 2012 Royal Society of Chemistry.

than that of materials produced by hydrothermal reduction, likely due to a more complete reduction and restoration of  $\pi$ -conjugation. Nearly concurrently, the chemical reduction approach has been reported by several groups to be an effective strategy to realize the 3D self-assembly of graphene, although with different reducing reagents such as ascorbic acid,  $\text{NaHSO}_3$ ,  $\text{Na}_2\text{S}$ , and HI.<sup>47,48</sup> The mild reaction conditions of the chemical reduction process can allow for preparation of graphene hydrogels modified with redox active anthraquinone through a two-step procedure in which anthraquinone covalently grafted GO was first synthesized and then chemically reduced by sodium ascorbate (Figure 2b,c).<sup>49</sup> After chemical reduction, only a small amount of anthraquinone was removed, and the chemically modified graphene hydrogels contained 16 wt % anthraquinone. To simplify the preparation procedure, we have further synthesized noncovalently functionalized graphene hydrogels through a convenient one-step chemical reduction of GO using hydroquinones as both the reducing and functionalizing molecules (Figure 2d).<sup>50</sup> The functionalized graphene hydrogels showed a high specific surface area of  $1380 \text{ m}^2/\text{g}$ , which could accommodate a large content of redox active hydroquinone molecules, up to 17 wt %, on the graphene surface via  $\pi$ - $\pi$  interactions. Similar to hydrothermal reduction, the chemical reduction strategy has also been widely used to prepare a variety of graphene composite hydrogels/aerogels with secondary components incorporated either before or during the self-assembly process.<sup>51–53</sup>

### 2.3. Electrochemical Reduction

Many applications of graphene, especially electrochemistry-related applications, require the deposition of graphene materials on electrodes. However, this is usually done by first synthesizing graphene active materials followed by coating of the mixture with polymer binders or conductive additives. Alternatively, a convenient electrochemical reduction strategy can be used to directly deposit 3D self-assembled graphene macrostructures on electrodes (Figure 3).<sup>54</sup> Typically, graphene hydrogels were electrodeposited on working electrode by electrolyzing a concentrated GO aqueous dispersion (3.0 mg/mL) containing 0.1 M  $\text{LiClO}_4$  at a potential of  $-1.2 \text{ V}$  vs saturated calomel electrode for tens of seconds in a three-electrode system. Under these conditions, the GO sheets near the electrode were electrochemically reduced and the resultant hydrophobic RGO sheets self-assembled on the electrode surface to form a well-bonded 3D porous network with most of the RGO sheets nearly vertically aligned to the electrode

surface. The thickness of graphene hydrogel film on the electrode was found to increase with the electrodeposition time and could reach several millimeters after long deposition time. The electrochemical reduction of GO can be carried out on different types of electrodes including graphene paper, nickel foam, and metal foil or fiber, which thus is a universal strategy for direct preparation of graphene hydrogels on electrodes.<sup>55,56</sup>

The porous graphene hydrogels on electrodes are conductive and highly accessible for electrolyte and thus can be used as a new electrode for further electrodeposition of secondary functional components such as conducting polymers, metal nanoparticles, and metal oxide onto the graphene porous network to make composite hydrogels.<sup>55</sup> For example, a graphene/polyaniline composite hydrogel can be readily prepared by a one-step cyclic voltammetry co-deposition process at a potential range of  $-1.2$  to  $0.8 \text{ V}$  in a mixture dispersion of GO and aniline, during which GO sheets were electrochemically reduced to form a graphene hydrogel layer on the substrate electrode at negative potential, and aniline monomers were polymerized and homogeneously coated on the surfaces of RGO sheets at positive potential.<sup>57</sup>

### 3. APPLICATIONS IN SUPERCAPACITORS

Supercapacitors, also known as electrochemical capacitors, represent an important kind of electrochemical energy storage device with high power density, long cycle life, and high rate capability.<sup>58</sup> The commercial supercapacitors are mainly based on activated carbon with unsatisfactory specific capacitances ( $<120 \text{ F/g}$ ) and relatively lower charge/discharge rates ( $<10 \text{ A/g}$ ). It is of considerable challenge to improve specific capacitance of the supercapacitor electrodes without sacrificing the rate performance or cycle life. The formation of 3D graphene network can effectively prevent graphene from restacking and retain the high specific surface area that is necessary for high specific capacitance. Additionally, with a highly interconnected graphene network for excellent electron transport and interpenetrated porous network for rapid ion transport, the 3D graphene macrostructures are ideally suited for supercapacitor electrodes.

We have first shown that graphene hydrogels prepared by hydrothermal reduction could be directly used as supercapacitor electrodes without any other additives and exhibited a high specific capacitance of  $175 \text{ F/g}$  in  $5 \text{ M KOH}$  electrolyte, about 45% higher than that of agglomerated RGO powders ( $120 \text{ F/g}$ ) under the same test conditions.<sup>28</sup> Subsequently, we improved the electrical conductivity and optimized the specific

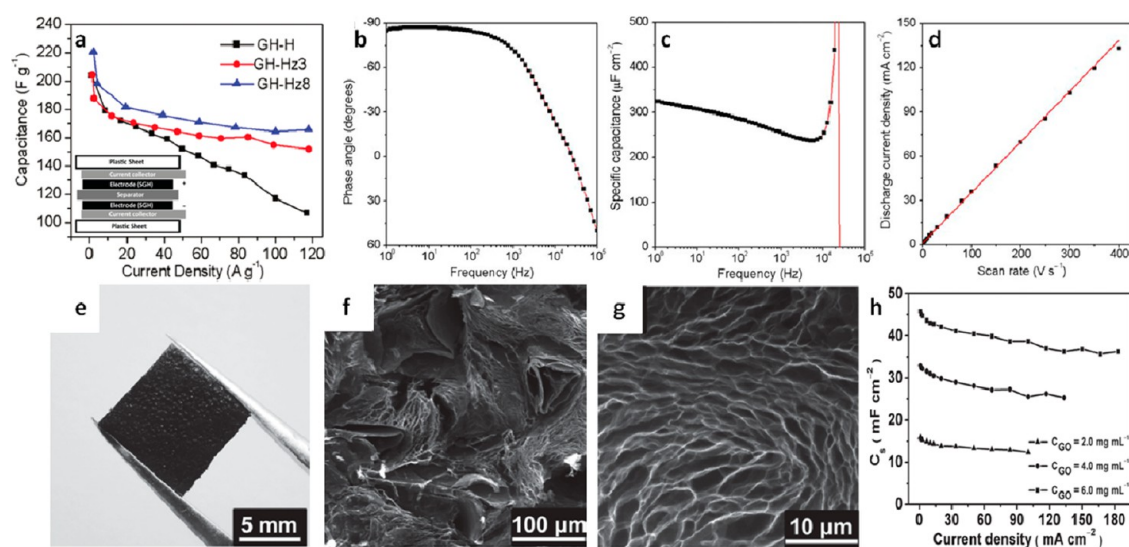


**Figure 4.** (a) Specific capacitance versus current density for graphene hydrogels prepared by hydrothermal reduction and further reduction by hydrazine for 3 and 8 h, respectively. Inset shows the schematic of graphene hydrogel-based supercapacitor. Reproduced with permission from ref 59. Copyright 2011 American Chemical Society. (b–d) Electrochemical characterization of supercapacitor based on electrodeposited graphene hydrogel thin film. (b) Plot of impedance phase angle versus frequency. (c) Plot of areal capacitance versus frequency using a series-RC circuit model. (d) Evolution of the discharge current density versus scan rate. Reproduced with permission from ref 54. Copyright 2012 Nature Publishing Group. (e–h) Structure and electrochemical characterization of graphene hydrogel deposited in nickel foam electrode. (e) Photograph of a piece electrode. (f) Low- and (g) high-magnification SEM images of a freeze-dried electrode. (h) Plots of areal capacitance versus current density for the electrodes prepared by chemical reduction of GO dispersions with different concentrations. Reproduced with permission from ref 60. Copyright 2012 Wiley-VCH.

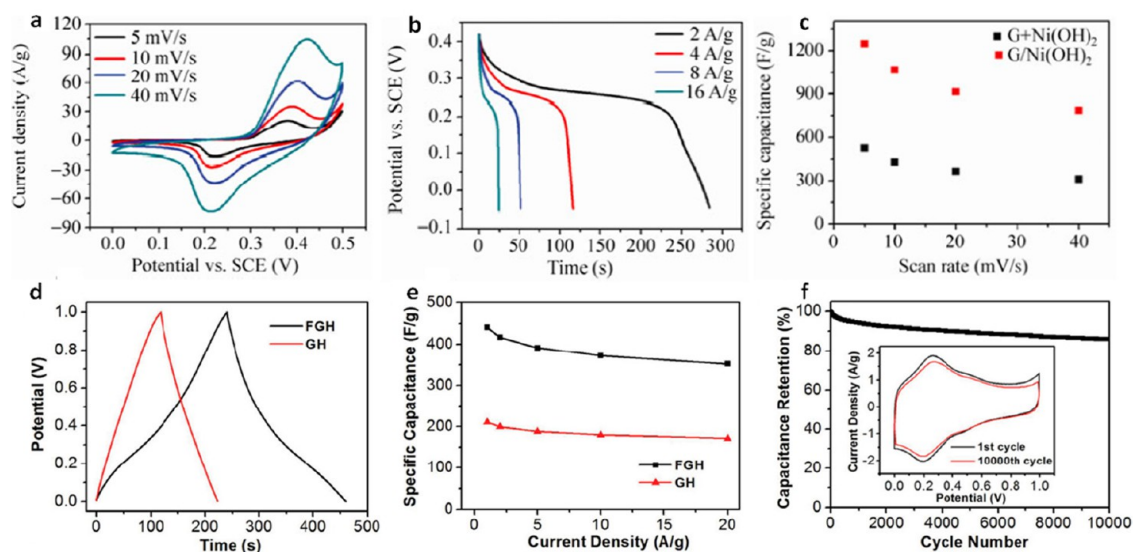


**Figure 5.** (a–c) Electrochemical characterization of graphene/ $\text{Ni}(\text{OH})_2$  composite hydrogel. Cyclic voltammety (a) and galvanostatic discharge (b) curves. (c) Specific capacitance versus current density for graphene/ $\text{Ni}(\text{OH})_2$  composite hydrogel and powdery mixture of graphene and  $\text{Ni}(\text{OH})_2$ , respectively. Reproduced with permission from ref 30. Copyright 2013 Springer Ltd. (d–f) Electrochemical characterization of hydroquinone functionalized graphene hydrogel. Galvanostatic charge/discharge curves at 1 A/g (d) and specific capacitance versus current density (e) for hydroquinone functionalized graphene hydrogel and pure graphene hydrogel, respectively. (f) Cycling stability at a current density of 10 A/g. Reproduced with permission from ref 50. Copyright 2013 Wiley-VCH.

capacitance up to 222 F/g at 1 A/g by further chemical reduction of the graphene hydrogels with hydrazine (Figure 4a).<sup>59</sup> Most importantly, the graphene hydrogels showed an excellent rate capability with a capacitance retention of 74% at an ultrahigh discharge rate of 100 A/g and a superior cycling stability with 92% capacitance remained after 20 000 charging/discharging cycles, which could be attributed to rapid ion diffusion and fast electron transport throughout the entire porous network of graphene hydrogels. We have also tested the

graphene hydrogels prepared by chemical reduction with sodium ascorbate and achieved similar capacitive performances with a high specific capacitance of 240 F/g in 1 M  $\text{H}_2\text{SO}_4$  electrolyte.<sup>46</sup>

Inspired by these exciting results, we have further fabricated an ultrahigh-rate supercapacitor based on graphene hydrogel thin film electrodes by electrochemical reduction strategy for alternating current line-filtering (Figure 4b–d).<sup>54</sup> The electrodes with  $\sim 20$   $\mu\text{m}$ -thick oriented graphene porous structures

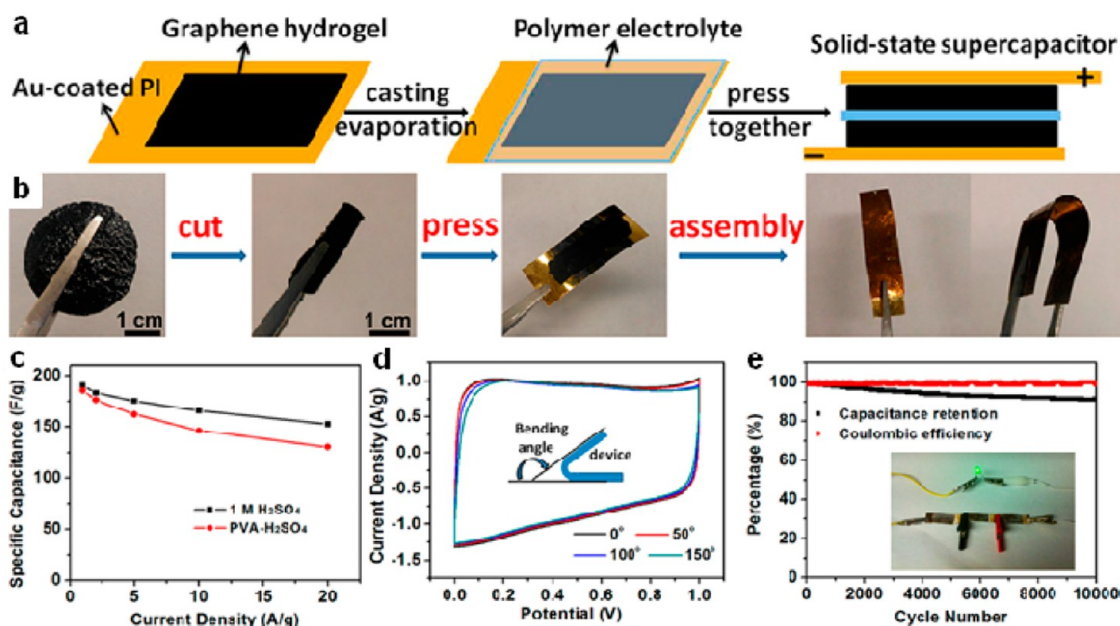


**Figure 6.** Schematic illustration (a) and photographs (b) of the fabrication process of flexible solid-state supercapacitors based on graphene hydrogel films. (c) Comparison of specific capacitances of graphene hydrogel film electrode in polymer gel electrolyte and in 1 M H<sub>2</sub>SO<sub>4</sub> electrolyte. (d) Cyclic voltammetry curves of the flexible solid-state device at 10 mV/s under different bending angles. (e) Cycling stability of the device at a current density of 10 A/g. The inset shows a green LED powered by the three supercapacitors in series. Reproduced with permission from ref 63. Copyright 2013 American Chemical Society.

exhibited a phase angle as large as  $-84^\circ$ , and a very short resistor–capacitor time of 1.35 ms along with a high areal capacitance of  $283 \mu\text{F}/\text{cm}^2$  at 120 Hz, which make the device capable of replacing the commercial aluminum electrolytic capacitor for 120 Hz line-filtering. We have also grown graphene hydrogels in the macropores of nickel foam by in situ chemical reduction of GO to form a double-network graphene hydrogel/nickel foam electrode (Figure 4e–h).<sup>60</sup> In this case, the whole graphene hydrogel was interpenetrated by the nickel framework, different from traditional electrode configuration in which graphene materials are attached onto a flat current collector. The increased contact between the graphene hydrogel and nickel foam brought about a significantly improved ion/electron transport dynamics within the electrode. Consequently, the electrode exhibited a large areal capacitance of  $46 \text{ mF}/\text{cm}^2$  at a current density of  $0.67 \text{ mA}/\text{cm}^2$  and a remarkable rate performance with a capacitance retention of 80% at an ultrahigh current density of  $183 \text{ mA}/\text{cm}^2$ , which is at least 1 order of magnitude higher than those of other high-rate supercapacitors based on onion-like carbon ( $1.7 \text{ mF}/\text{cm}^2$  at  $1 \text{ V}/\text{s}$ )<sup>61</sup> and laser-scribed graphene ( $3.67 \text{ mF}/\text{cm}^2$  at  $36.3 \mu\text{A}/\text{cm}^2$ ).<sup>62</sup>

Pseudocapacitive materials such as conducting polymers and electrochemically active metal oxides (or hydroxides) can exhibit much higher theoretical specific capacitance than carbon materials but typically suffer from low electrical conductivity and poor cycling stability. Incorporation of these pseudocapacitive materials into the 3D graphene macrostructures has the potential to take advantage of both components to achieve greatly improved overall performance. We have utilized a one-step hydrothermal strategy to prepare graphene/Ni(OH)<sub>2</sub> composite hydrogels in which ultrathin Ni(OH)<sub>2</sub> nanoplates were grown uniformly on the surface of graphene sheets during the formation of the 3D graphene framework.<sup>30</sup> The composite hydrogels showed high specific capacitances of 1212 and 813

F/g at current densities of 2 and 16 A/g, respectively, and  $\sim 95\%$  capacitance retention after 2000 cycle tests, which are superior to most of the powdery graphene/Ni(OH)<sub>2</sub> composites reported (Figure 5a–c). We have also incorporated redox active hydroquinone into the 3D graphene macrostructures by simultaneous chemical reduction and functionalization of GO with hydroquinone and achieved a significantly improved specific capacitance of 441 F/g compared with 221 F/g for pure graphene hydrogels and an excellent rate capability with a capacitance retention of 80% at 20 A/g, as well as superior cycling stability with a capacitance retention of 86% over 10 000 cycles (Figure 5d–f).<sup>50</sup> Interestingly, the pseudocapacitance contributed by hydroquinone was calculated to be 1461 F/g, about 83% of its theoretical value (1751 F/g), indicating a highly efficient utilization of adsorbed hydroquinone. The overall capacitive performances of the hydroquinone functionalized graphene hydrogels are better than many other chemically modified graphene materials, which is mainly ascribed to a large amount of hydroquinone molecules loaded on the high-surface-area 3D graphene framework and rapid charge transfer between graphene substrate and hydroquinone, which is tightly adsorbed on graphene via  $\pi$ – $\pi$  interactions. Meanwhile, a graphene/polyaniline composite hydrogel film has also been prepared by an electrochemical co-deposition approach to greatly increase the areal capacitance of the high-rate supercapacitor from  $487 \mu\text{F}/\text{cm}^2$  to  $12.4 \text{ mF}/\text{cm}^2$  with the rate capability well maintained (93% capacitance retention from 0.5 to 50 mA/cm<sup>2</sup>).<sup>57</sup> Other groups have also demonstrated that heteroatom-doping of 3D graphene macrostructures is another effective method to modify the electronic structure and surface wetting to improve their capacitive performance.<sup>32–34</sup>

With flexible and wearable electronics becoming increasingly popular in our daily life, there is a great need for flexible electrochemical energy storage devices. Our recent study

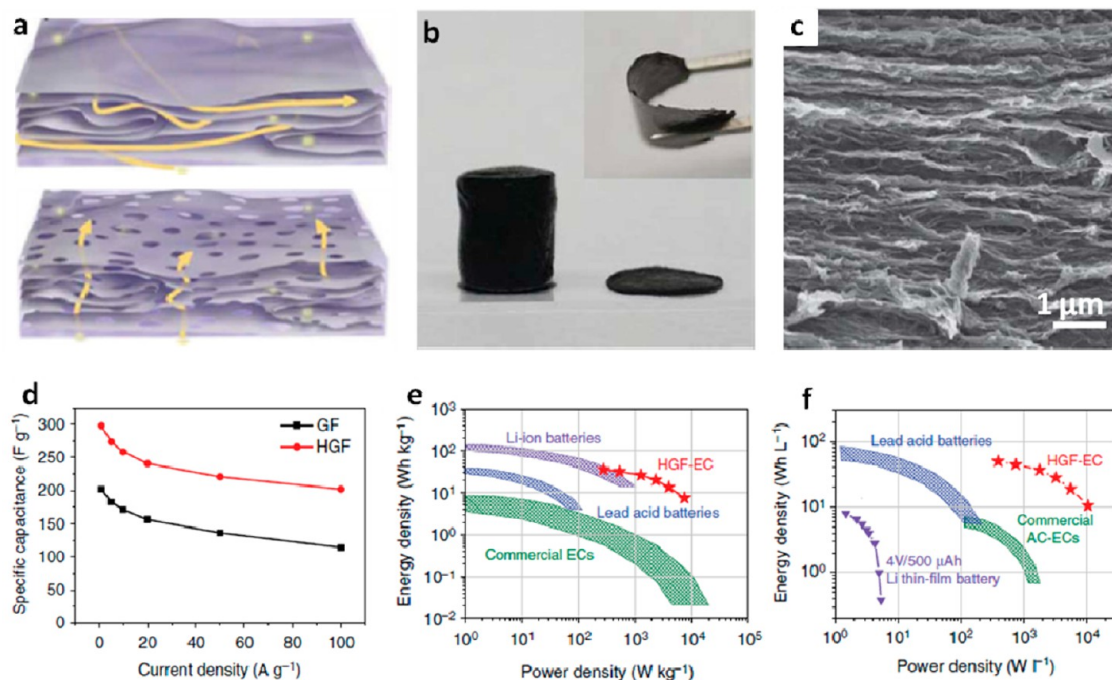


**Figure 7.** (a) Schematic illustration of ion diffusion pathway across the graphene framework (top) and holey graphene framework (bottom) films. (b) Photographs showing holey graphene framework before and after mechanical compression with the flexibility of the film shown in the inset. (c) Cross-sectional SEM image of the compressed holey graphene framework film. (d) Specific capacitance versus current density. (e, f) Ragone plots of gravimetric energy density versus gravimetric power density (e) and volumetric energy density versus volumetric power density (f) for holey graphene framework film based supercapacitor in comparison with lead-acid batteries, lithium-ion battery, and commercial supercapacitors. The energy and power densities are normalized by the weight or volume of the entire device stack. Reproduced with permission from ref 45. Copyright 2014 Nature Publishing Group.

demonstrated that flexible solid-state supercapacitors with 120- $\mu\text{m}$  thick graphene hydrogel films as electrodes could exhibit a high specific capacitance of 196 F/g, an unprecedented areal capacitance of 402 mF/cm<sup>2</sup>, a low leakage current of 10.6  $\mu\text{A}$ , excellent cycling stability with only 8.4% capacitance decay over 10 000 charge/discharge cycles, and extraordinary mechanical flexibility (Figure 6).<sup>63</sup> Subsequently, we have also fabricated a flexible solid-state device based on hydroquinone functionalized graphene hydrogels with an improved specific capacitance of 412 F/g and other similarly superior capacitive characteristics.<sup>50</sup> These results represent notable progress compared with previous solid-state devices based on carbon nanotubes and graphene film (<120 F/g and <50 mF/cm<sup>2</sup>) and signify the exciting potential of 3D graphene macrostructures for high-performance flexible energy storage devices. We have also extended the configuration of the solid-state supercapacitors from 2D film to 1D fiber by electrodeposition of graphene hydrogels on metal wires as the electrode material.<sup>56</sup> The fiber-like device delivered a higher areal capacitance of 6.5 mF/cm<sup>2</sup> than previous fiber-shaped supercapacitors (usually below 3 mF/cm<sup>2</sup>) and showed excellent mechanical flexibility.

For many practical applications with limited space, the volumetric performance of supercapacitor electrodes is becoming an increasingly important metric to consider. However, there is usually a trade-off relationship between the gravimetric and volumetric capacitances for most electrode designs. Highly porous electrodes can boost specific surface area and favor ion diffusion for high gravimetric capacitance but usually with poor volumetric capacitance due to its relatively low packing density, while a more compact electrode may increase the volumetric capacitance but decrease the ion-

accessible surface area and ion diffusion rate resulting in a low gravimetric capacitance and poor rate performance. To this end, we have recently created a 3D holey graphene framework that can be compressed into a densely packed film to simultaneously achieve high packing density, large ion accessible surface area, and fast ion transport rate.<sup>45</sup> Particularly, the abundant nanopores created in the holey graphene sheet not only increase the specific surface area but also can function as the ion diffusion shortcuts between different layers of graphene to greatly speed up the ion transport and facilitate ion access to the entire surface area even in the highly compressed state (Figure 7a–c). With this unique design, the compressed holey graphene framework showed ultrahigh gravimetric and volumetric capacitances of 298 F/g and 212 F/cm<sup>3</sup>, both being the highest values achieved in organic electrolytes to date (Figure 7d). Furthermore, we showed that a packaged device stack could deliver gravimetric and volumetric energy densities of 35 Wh/kg and 49 Wh/L, respectively, approaching those of lead acid batteries (25–35 Wh/kg and 50–90 Wh/L) (Figure 7e,f).

#### 4. CONCLUSIONS

This Account summarizes our recent advances in synthesis of 3D self-assembled graphene macrostructures and their applications in supercapacitors. With diverse synthetic strategies developed, a wide range of advanced 3D graphene materials can be readily prepared on a large scale and show great potential as binder-free electrodes in supercapacitors with significantly improved performance compared with previous carbon nanomaterials and powdery graphene materials. Beyond this exciting progress to date, we believe there are considerable

challenges and opportunities remaining for continued investigation. First, the current 3D self-assembled graphene macrostructures are generally based on RGO sheets with a relatively poor electrical quality and a wide polydispersibility in physical morphology and chemical structure, which results in relatively low electrical properties of the resultant 3D materials and insufficient understanding of the structure–property relationship. Second, the intrinsic microstructures and species diffusion within the 3D graphene framework are partly unclear and need to be further investigated to enhance the material performance. Third, more functional components can be rationally introduced into the 3D graphene macrostructures to further expand the functions and applications of the 3D graphene materials. Finally, 3D graphene macrostructures that simultaneously exhibit stretchability, flexibility, and compressibility have not been realized so far but are highly desired for powering smart and wearable electronic products. With the multidisciplinary efforts from chemistry, physics, biology, and materials science, as well as a combination of many unique attributes, we believe that the self-assembled 3D graphene materials could open up significant technological opportunities in diverse areas and in the near future.

## AUTHOR INFORMATION

### Corresponding Authors

\*Gaoquan Shi. E-mail: gshi@tsinghua.edu.cn.

\*Xiangfeng Duan. E-mail: xduan@chem.ucla.edu.

### Author Contributions

The manuscript was written through contributions of all authors. All authors have given approval to the final version of the manuscript.

### Funding

X.D. acknowledges support from the U.S. Department of Energy, Office of Basic Energy Sciences, Division of Materials Science and Engineering, through Award DE-SC0008055. G.S. acknowledges partial support by the National Basic Research Program of China (Grants 2012CB933402, 2013CB933001) and the Natural Science Foundation of China (Grant 51433005).

### Notes

The authors declare no competing financial interest.

### Biographies

**Yuxi Xu** received his B.S. degree in Chemistry from Wuhan University (2007) and Ph.D. degree in Chemistry from Tsinghua University (2011). He is currently working as a postdoctoral researcher in the group of Prof. Xiangfeng Duan at University of California, Los Angeles. His current work focuses on the synthesis and applications of self-assembled graphene materials. His research interests include conjugated polymers, carbon nanomaterials, and self-assembly chemistry.

**Gaoquan Shi** received his B.S. degree (1985) and Ph.D. degree (1992) in the Department of Chemistry at Nanjing University. Then he joined Nanjing University and was promoted to full professor in 1995. In 2000, he moved to Tsinghua University. His research interests are focused on synthesis and application of conducting polymers and graphene.

**Xiangfeng Duan** is currently a Professor in the Department of Chemistry and Biochemistry at UCLA. He received his B.S. in Chemistry from USTC, China (1997), and his M.A. degree in

Chemistry (1999) and Ph.D. in Physical Chemistry (2002) from Harvard University. He was previously a founding scientist at Nanosys Inc. His current research interests include nanoscale materials and devices for future electronics, energy, and biomedical sciences.

## REFERENCES

- (1) Novoselov, K. S.; Geim, A. K.; Morozov, S. V.; Jiang, D.; Zhang, Y.; Dubonos, S. V.; Grigorieva, I. V.; Firsov, A. A. Electric field effect in atomically thin carbon films. *Science* **2004**, *306*, 666–669.
- (2) Weiss, N. O.; Zhou, H. L.; Liao, L.; Liu, Y.; Jiang, S.; Huang, Y.; Duan, X. F. Graphene: An emerging electronic material. *Adv. Mater.* **2012**, *24*, 5782–5825.
- (3) Novoselov, K. S.; Fal'co, V. I.; Colombo, L.; Gellert, P. R.; Schwab, M. G.; Kim, K. A roadmap for graphene. *Nature* **2012**, *490*, 192–200.
- (4) Huang, X.; Qi, X. Y.; Boey, F.; Zhang, H. Graphene-based composites. *Chem. Soc. Rev.* **2012**, *41*, 666–686.
- (5) Huang, X.; Zeng, Z.; Fan, Z.; Liu, J.; Zhang, H. Graphene-based electrodes. *Adv. Mater.* **2012**, *24*, 5979–6004.
- (6) Yin, Z.; Zhu, J.; He, Q.; Cao, X.; Tan, C.; Chen, H.; Yan, Q.; Zhang, H. Graphene-based materials for solar cell applications. *Adv. Energy Mater.* **2014**, *4*, No. 1300574.
- (7) Li, X.; Cai, W.; An, J.; Kim, S.; Nah, J.; Yang, D.; Piner, R.; Velamakanni, A.; Jung, I.; Tutuc, E.; Banerjee, S. K.; Colombo, L.; Ruoff, R. S. Large-area synthesis of high-quality and uniform graphene films on copper foils. *Science* **2009**, *324*, 1312–1314.
- (8) Park, S.; Ruoff, R. S. Chemical methods for the production of graphenes. *Nat. Nanotechnol.* **2009**, *4*, 217–224.
- (9) Xu, Y. X.; Shi, G. Q. Assembly of chemical modified graphene: Methods and applications. *J. Mater. Chem.* **2011**, *21*, 3311–3323.
- (10) Kim, J.; Cote, L. J.; Huang, J. X. Two dimensional soft material: New faces of graphene oxide. *Acc. Chem. Res.* **2012**, *45*, 1356–1364.
- (11) Wu, D. Q.; Zhang, F.; Liang, H.; Feng, X. L. Nanocomposites and macroscopic materials: Assembly of chemically modified graphene sheets. *Chem. Soc. Rev.* **2012**, *41*, 6160–6177.
- (12) Xu, Y. X.; Bai, H.; Lu, G. W.; Li, C.; Shi, G. Q. Flexible graphene films via the filtration of water-soluble noncovalent functionalized graphene sheets. *J. Am. Chem. Soc.* **2008**, *130*, 5856–5857.
- (13) Xu, Y. X.; Zhao, L.; Bai, H.; Hong, W. J.; Li, C.; Shi, G. Q. Chemically converted graphene induced molecular flattening of 5,10,15,20-tetrakis(1-methyl-4-pyridinio)porphyrin and its application for optical detection of cadmium(II) ions. *J. Am. Chem. Soc.* **2009**, *131*, 13490–13497.
- (14) Xu, Y. X.; Hong, W. J.; Bai, H.; Li, C.; Shi, G. Q. Strong and ductile poly(vinyl alcohol)/graphene oxide composite films with a layered structure. *Carbon* **2009**, *47*, 3538–3543.
- (15) Xu, Y. X.; Wu, Q.; Sun, Y. Q.; Bai, H.; Shi, G. Q. Three-dimensional self-assembly of graphene oxide and DNA into multi-functional hydrogels. *ACS Nano* **2010**, *4*, 7358–7362.
- (16) Wu, Q.; Xu, Y. X.; Yao, Z. Y.; Liu, A. R.; Shi, G. Q. Supercapacitors based on flexible graphene/polyaniline nanofiber composite films. *ACS Nano* **2010**, *4*, 1963–1970.
- (17) Xue, T.; Jiang, S.; Qu, Y. Q.; Su, Q.; Cheng, R.; Dubin, S.; Chiu, C.-Y.; Kaner, R.; Huang, Y.; Duan, X. F. Graphene-supported hemin as a highly active biomimetic oxidation catalyst. *Angew. Chem., Int. Ed.* **2012**, *51*, 3822–3825.
- (18) Xue, T.; Peng, B.; Xue, M.; Zhong, X.; Chiu, C. Y.; Yang, S.; Qu, Y. Q.; Ruan, L. Y.; Jiang, S.; Dubin, S.; Kaner, R. B.; Zink, J. I.; Meyerhoff, M. E.; Duan, X. F.; Huang, Y. Integration of molecular and enzymatic catalysts on graphene for biomimetic generation of antithrombotic species. *Nat. Commun.* **2014**, *5*, No. 3200.
- (19) Jiang, S.; Cheng, R.; Wang, X.; Xue, T.; Liu, Y.; Nel, A.; Huang, Y.; Duan, X. F. Real-time electrical detection of nitric oxide in biological systems with sub-nanomolar sensitivity. *Nat. Commun.* **2013**, *4*, No. 2225.
- (20) Whittingham, M. S. History, evolution, and future status of energy storage. *Proc. IEEE* **2012**, *100*, 1518–1534.



- (21) Sun, Y. Q.; Wu, Q.; Shi, G. Q. Graphene based new energy materials. *Energy Environ. Sci.* **2011**, *4*, 1113–1132.
- (22) Li, C.; Shi, G. Q. Three-dimensional graphene architectures. *Nanoscale* **2012**, *4*, 5549–5563.
- (23) Yin, S.; Niu, Z.; Chen, X. Assembly of graphene sheets into 3D macroscopic structures. *Small* **2012**, *8*, 2458–2463.
- (24) Li, C.; Shi, G. Q. Functional gels base chemically modified graphene. *Adv. Mater.* **2014**, *26*, 3392–4012.
- (25) Cao, X.; Yin, Z.; Zhang, H. Three-dimensional graphene materials: preparation, structures and application in supercapacitors. *Energy Environ. Sci.* **2014**, *7*, 1850–1865.
- (26) Zhou, W.; Cao, X.; Zeng, Z.; Shi, W.; Zhu, Y.; Yan, Q.; Liu, H.; Wang, J.; Zhang, H. One-step synthesis of Ni<sub>3</sub>S<sub>2</sub> nanorod@Ni(OH)<sub>2</sub> nanosheet core-shell nanostructures on a three-dimensional graphene network for high-performance supercapacitors. *Energy Environ. Sci.* **2013**, *6*, 2216–2221.
- (27) Cao, X.; Shi, Y.; Shi, W.; Liu, G.; Huang, X.; Yan, Q.; Zhang, Q.; Zhang, H. Preparation of novel 3D graphene networks for supercapacitor applications. *Small* **2011**, *7*, 3163–3168.
- (28) Xu, Y. X.; Sheng, K. X.; Li, C.; Shi, G. Q. Self-assembled graphene hydrogel via a one-step hydrothermal process. *ACS Nano* **2010**, *4*, 4324–4330.
- (29) Sun, Y. Q.; Wu, Q.; Shi, G. Q. Supercapacitors based on self-assembled graphene organogel. *Phys. Chem. Chem. Phys.* **2011**, *13*, 17249–17254.
- (30) Xu, Y. X.; Huang, X. Q.; Lin, Z. Y.; Zhong, X.; Huang, Y.; Duan, X. F. One-step strategy to graphene/Ni(OH)<sub>2</sub> composite hydrogels as advanced three-dimensional supercapacitor electrode materials. *Nano Res.* **2013**, *6*, 65–76.
- (31) Zhou, Q. Q.; Gao, J.; Li, C.; Chen, J.; Shi, G. Q. Composite organogels of graphene and activated carbon for electrochemical capacitors. *J. Mater. Chem. A* **2013**, *1*, 9196–9201.
- (32) Wu, Z. S.; Winter, A.; Chen, L.; Sun, Y.; Turchanin, A.; Feng, X. L.; Mullen, K. Three-dimensional nitrogen and boron co-doped graphene for high-performance all-solid-state supercapacitors. *Adv. Mater.* **2012**, *24*, 5130–5135.
- (33) Zhao, Y.; Hu, C.; Hu, Y.; Cheng, H.; Shi, G.; Qu, L. A versatile, ultralight, nitrogen-doped graphene framework. *Angew. Chem., Int. Ed.* **2012**, *51*, 11371–11375.
- (34) Chen, P.; Yang, J. J.; Li, S. S.; Wang, Z.; Xiao, T. Y.; Qian, Y. H.; Yu, S. H. Hydrothermal synthesis of macroscopic nitrogen-doped graphene hydrogels for ultrafast supercapacitor. *Nano Energy* **2013**, *2*, 249–256.
- (35) Wang, Y.; Wu, Y.; Huang, Y.; Zhang, F.; Yang, X.; Ma, Y.; Chen, Y. Preventing graphene sheets from restacking for high-capacitance performance. *J. Phys. Chem. C* **2011**, *115*, 23192–23197.
- (36) Ai, L.; Jiang, J. Removal of methylene blue from aqueous solution with self-assembled cylindrical graphene-carbon nanotube hybrid. *Chem. Eng. J.* **2012**, *192*, 156–163.
- (37) Liu, J.; Wang, Z.; Zhao, Y.; Cheng, H.; Hu, C.; Jiang, L.; Qu, L. Three-dimensional graphene-polyppyrole hybrid electrochemical actuator. *Nanoscale* **2012**, *4*, 7563–7568.
- (38) Zhao, Y.; Zhao, F.; Wang, X. P.; Xu, C. Y.; Zhang, Z. P.; Shi, G. Q.; Qu, L. T. Graphitic carbon nitride nanoribbons: Graphene-assisted formation and synergic function for highly efficient hydrogen evolution. *Angew. Chem., Int. Ed.* **2014**, *53*, 13934–13939.
- (39) Tang, Z.; Shen, S.; Zhuang, J.; Wang, X. Noble-metal-promoted three-dimensional macroassembly of single-layered graphene oxide. *Angew. Chem., Int. Ed.* **2010**, *49*, 4603–4607.
- (40) Hu, C.; Zhao, Y.; Cheng, H.; Hu, Y.; Shi, G.; Dai, L.; Qu, L. Ternary Pd<sub>2</sub>/PtFe networks supported by 3D graphene for efficient and durable electrooxidation of formic acid. *Chem. Commun.* **2012**, *48*, 11865–11867.
- (41) Hu, C.; Cheng, H.; Zhao, Y.; Hu, Y.; Liu, Y.; Dai, L.; Qu, L. Newly-designed complex ternary Pt/PdCu nanoboxes anchored on three-dimensional graphene framework for highly efficient ethanol oxidation. *Adv. Mater.* **2012**, *24*, 5493–5498.
- (42) Wu, Z. S.; Yang, S.; Sun, Y.; Parvez, K.; Feng, X.; Müllen, K. 3D nitrogen-doped graphene aerogel-supported Fe<sub>3</sub>O<sub>4</sub> nanoparticles as efficient electrocatalysts for the oxygen reduction reaction. *J. Am. Chem. Soc.* **2012**, *134*, 9082–9085.
- (43) Gong, Y.; Yang, S.; Liu, Z.; Ma, L.; Vajtai, R.; Ajayan, P. M. Graphene-network-backboned architectures for high-performance lithium storage. *Adv. Mater.* **2013**, *25*, 3979–3984.
- (44) Zhang, Z.; Xiao, F.; Guo, Y.; Wang, S.; Liu, Y. One-pot self-assembled three-dimensional TiO<sub>2</sub>-graphene hydrogel with improved adsorption capacities and photocatalytic and electrochemical activities. *ACS Appl. Mater. Interfaces* **2013**, *5*, 2227–2233.
- (45) Xu, Y. X.; Lin, Z. Y.; Zhong, X.; Huang, X. Q.; Weiss, N. O.; Huang, Y.; Duan, X. F. Holey graphene frameworks for highly efficient capacitive energy storage. *Nat. Commun.* **2014**, *5*, No. 4554.
- (46) Sheng, K. X.; Xu, Y. X.; Li, C.; Shi, G. Q. High-performance self-assembled graphene hydrogels prepared by chemical reduction of graphene oxide. *New Carbon Mater.* **2011**, *26*, 9–15.
- (47) Chen, W. F.; Yan, L. F. In situ self-assembly of mild chemical reduction graphene for three-dimensional architectures. *Nanoscale* **2011**, *3*, 3132–3137.
- (48) Zhang, X. T.; Sui, Z. Y.; Xu, B.; Yue, S. F.; Luo, Y. J.; Zhan, W. C.; Liu, B. Mechanically strong and highly conductive graphene aerogel and its use as electrodes for electrochemical power sources. *J. Mater. Chem.* **2011**, *21*, 6494–6497.
- (49) Wu, Q.; Sun, Y. Q.; Bai, H.; Shi, G. Q. High-performance supercapacitor electrodes based on graphene hydrogels modified with 2-aminoanthraquinone moieties. *Phys. Chem. Chem. Phys.* **2011**, *13*, 11193–11198.
- (50) Xu, Y. X.; Lin, Z. Y.; Huang, X. Q.; Wang, Y.; Huang, Y.; Duan, X. F. Functionalized graphene hydrogel-based high-performance supercapacitors. *Adv. Mater.* **2013**, *25*, 5779–5784.
- (51) Sui, Z. Y.; Zhang, X. T.; Lei, Y.; Luo, Y. J. Easy and green synthesis of reduced graphite oxide-based hydrogels. *Carbon* **2011**, *49*, 4314–4321.
- (52) Chen, W.; Li, S.; Chen, C.; Yan, L. Self-assembly and embedding of nanoparticles by in situ reduced graphene for preparation of a 3D graphene/nanoparticle aerogel. *Adv. Mater.* **2011**, *23*, 5679–5683.
- (53) Cong, H. P.; Ren, X. C.; Wang, P.; Yu, S. H. Macroscopic multifunctional graphene-based hydrogels and aerogels by a metal ion induced self-assembly process. *ACS Nano* **2012**, *6*, 2693–2703.
- (54) Sheng, K. X.; Sun, Y. Q.; Li, C.; Yuan, W. J.; Shi, G. Q. Ultrahigh-rate supercapacitors based on electrochemically reduced graphene oxide for ac line-filtering. *Sci. Rep.* **2012**, *2*, No. 247.
- (55) Chen, K.; Chen, L.; Chen, Y.; Bai, H.; Lei, L. Three-dimensional porous graphene-based composite materials: Electrochemical synthesis and application. *J. Mater. Chem.* **2012**, *22*, 20968–20976.
- (56) Li, Y. R.; Sheng, K. X.; Yuan, W. J.; Shi, G. Q. A high-performance flexible fibre-shaped electrochemical capacitor based on electrochemically reduced graphene oxide. *Chem. Commun.* **2013**, *49*, 291–293.
- (57) Zhou, Q. Q.; Li, Y. R.; Huang, L.; Li, C.; Shi, G. Q. Three-dimensional porous graphene/polyaniline composites for high-rate electrochemical capacitors. *J. Mater. Chem. A* **2014**, *2*, 17489–17494.
- (58) Simon, P.; Gogotsi, Y. Materials for electrochemical capacitors. *Nat. Mater.* **2008**, *7*, 845–854.
- (59) Zhang, L.; Shi, G. Q. Preparation of highly conductive graphene hydrogels for fabricating supercapacitors with high rate capability. *J. Phys. Chem. C* **2011**, *115*, 17206–17212.
- (60) Chen, J.; Sheng, K. X.; Luo, P. H.; Li, C.; Shi, G. Q. Graphene hydrogels deposited in nickel foams for high-rate electrochemical capacitors. *Adv. Mater.* **2012**, *24*, 4569–4573.
- (61) Pech, D.; Brunet, M.; Durou, H.; Huang, P. H.; Mochalin, V.; Gogotsi, Y.; Taberna, P. L.; Simon, P. Ultrahigh-power micrometre-sized supercapacitors based on onion-like carbon. *Nat. Nanotechnol.* **2010**, *5*, 651–654.
- (62) El-Kady, M. F.; Strong, V.; Dubin, S.; Kaner, R. B. Laser scribing of high-performance and flexible graphene-based electrochemical capacitors. *Science* **2012**, *335*, 1326–1330.

(63) Xu, Y. X.; Lin, Z. Y.; Huang, X. Q.; Liu, Y.; Huang, Y.; Duan, X. F. Flexible solid-state supercapacitors based on three-dimensional graphene hydrogel films. *ACS Nano* **2013**, *7*, 4042–4049.